International Journal of Mechanical Engineering and Applications
2023; 11(1): 1-8
http://www.sciencepublishinggroup.com/j/ijmea
doi: 10.11648/j.ijmea.20231101.11
ISSN: 2330-023X (Print); ISSN: 2330-0248 (Online)

Quality Evaluation Method of Anchor Chain Flash Butt Welding Based on Deep Learning

Jiahe Gao, Haibo Wen, Shenao Zhu, Shihui Dong, Shijie Su*, Jian Zhang

School of Mechanical Engineering, Jiangsu University of Science and Technology, Zhenjiang, China

Email address:

sushijie@just.edu.cn (Shijie Su)

*Corresponding author

To cite this article:

Jiahe Gao, Haibo Wen, Shenao Zhu, Shihui Dong, Shijie Su, Jian Zhang. Quality Evaluation Method of Anchor Chain Flash Butt Welding Based on Deep Learning. *International Journal of Mechanical Engineering and Applications*. Vol. 11, No. 1, 2023, pp. 1-8.
doi: 10.11648/j.ijmea.20231101.11

Received: December 24, 2022; **Accepted**: January 10, 2023; **Published**: January 17, 2023

Abstract: Flash butt welding, a mainstream welding method employed in producing anchor chains, is a critical manufacturing process affecting the quality of anchor chains. Ultrasonic and load testing are used to evaluate the welding quality of anchor chains, but the cost of checking and replacing unqualified chain links is high. A deep learning-based quality evaluation method for flash butt welding is proposed to reduce the cost of detecting and replacing substandard chain links. First, displacement and current sensors collect electrode position and current signals during welding. Second, since the number of qualified anchor links is much larger than that of unqualified ones, a new data synthesis method is proposed: nearest-neighbor splicing sampling, which achieves the enhancement of minority samples by segmenting and combining existing data samples according to the features of anchor chain welding. Then, a piecewise linear interpolation method is used to handle the varying data length problem, thus satisfying the input requirements of the convolutional neural network (CNN). Finally, a CNN model is established, and dropout is used to reduce the over-fitting phenomenon. The experimental results show that the accuracy of the under-sampling method, over-sampling method, and nearest-neighbor splicing sampling method are 93.8%, 95.9%, and 96.3%, respectively, and the sensitivity, specificity, and accuracy of the CNN model are 95.7%, 93%, and 94.3%, respectively, which are better than those of the support vector machine (SVM).

Keywords: Deep Learning, Quality Evaluation, Anchor Chain, Flash Butt Welding, Nearest-Neighbor Splicing Sampling

1. Introduction

As necessary equipment for ensuring the safety of ships and offshore structures' safety, the industry has widely valued anchor chain quality. Since flash butt welding is a critical process in manufacturing anchor chains, the welding quality determines whether the mechanical properties of the finished anchor chain are qualified [1]. Due to the complex physical and chemical reactions in the flash butt welding process, it is difficult to establish an accurate welding quality evaluation model for evaluating whether the welding process is working correctly [2].

Recently, rapid development has been made in deep learning technology, represented by a deep neural network, widely used in image classification, speech recognition, and anomaly detection [3-7]. Some researchers have tried to use the deep learning algorithm to evaluate the welding quality by classifying the welded images to obtain preliminary research results. For example, Park et al. proposed a method based on a convolutional neural network (CNN) to inspect welding defects on the surface of an engine transmission with an accuracy of 99.3% [8]. Du et al. used CNN to identify the types of weld seams in gas-metal arc welding [9]. They achieved 98.0% classification accuracy through the purpose-built visual sensing system and fast segmentation of images.

Unlike standard arc welding, the welding joints of the anchor chain after flash butt welding is closed in the chain links, and valuable welding images can not be obtained. Therefore, this study evaluates the welding quality according to the change in sensing data in the flash butt welding process. The deep learning algorithm shows advantages for the classification of time series (e.g. sensing data of the welding process) [10]. For instance, Ronao et al. proposed a human activity recognition method based on a deep neural network with an accuracy of 95.8% [11]. Zhao et al. recognized speech emotion based on a merged deep

CNN with 92.7% accuracy [12]. Acharya et al. used CNN to automatically diagnose coronary artery diseases based on ECG signals, with 95.1% accuracy [13].

However, unlike the existing time series, the flash butt welding process's sensing data has multidimensionality characteristics, varying data length, and imbalanced datasets, making data pre-processing complicated. According to the features of flash butt welding of an anchor chain, this paper proposes a new method of welding quality evaluation based on the characteristic change of sensing data in the welding process and deep learning. A nearest-neighbor splicing sampling method for generating new samples is designed to handle the extreme imbalance of welding data issues. A sample is constantly selected from the unqualified samples, and the two samples closest to the selected sample are found to be spliced into a new sample. After piecewise linear interpolation and normalization of the samples, the CNN model is established and compared with the SVM. The experimental results show that the proposed welding quality evaluation method achieves 94.3% accuracy, which implies better recognition ability.

2. Research Method and Experimental Design

2.1. Flash Butt Welding of Anchor Chain

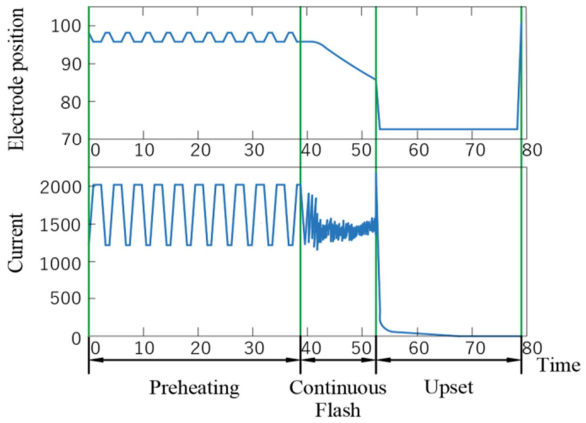

Figure 1. *Electrode position and current signal.*

Flash butt welding uses resistance heat supplied by a welding transformer to heat the two conjugate faces of an anchor chain to a suitable temperature and form a weld pool. Under upset force, the two conjugate faces are rapidly squeezed together, and fractions of the weld pool extrude. Figure 1 is an example of sampling the electrode position and current signals during an anchor chain welding process.

Figure 2 shows the process diagram of flash butt welding of anchor chain, including three main stages: preheating, continuous flash, and upset [1].

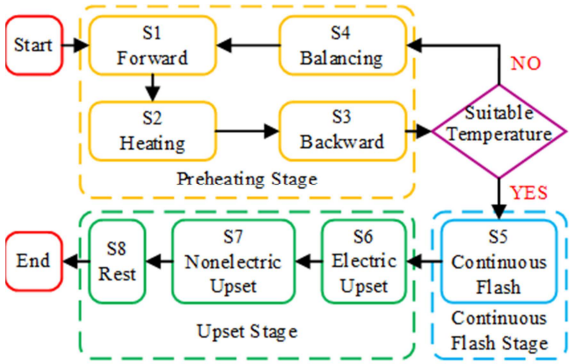

Figure 2. *Process diagram of flash butt welding of anchor chain.*

The preheating stage consists of the forward stage S1, heating stage S2, backward stage S3, and balancing stage S4. Stage S1 makes the two conjugate faces contact, stage S2 heats the conjugate faces, stage S3 separates the conjugate faces, and stage S4 causes the heat on the conjugate faces to diffuse into the metal. These four stages are repeated several times until the two conjugate faces reach a suitable temperature distribution.

In the continuous flash stage S5, the movable platen of the welding machine keeps moving forward with a suitable speed that matches the molten metal expelled speed, then generating a continuous flash between the two conjugate faces of an anchor chain link.

The upset stage includes the electric upset stage S6, the nonelectric upset stage S7, and the reset stage S8. At the beginning of the upset, a large upset force is applied to the anchor chain link to make the two conjugate faces close quickly and produce a certain plastic deformation to ensure the recrystallization of the weld joints. The electrode is charged while entering the upset stage to prevent high-temperature oxidation of the weld joints. Thus, the upset stage can be divided into electric and nonelectric. Finally, the electrode is reset to the initial position.

2.2. CNN

Convolutional neuro network (CNN), a famous deep learning algorithm, is used in many fields. The input of the neuro network is usually a two-dimensional matrix such as an image, but the electrode position and current in this paper are typical one-dimensional signals. Therefore, a one-dimensional CNN is established to evaluate the quality of anchor chain flash welding [14, 15].

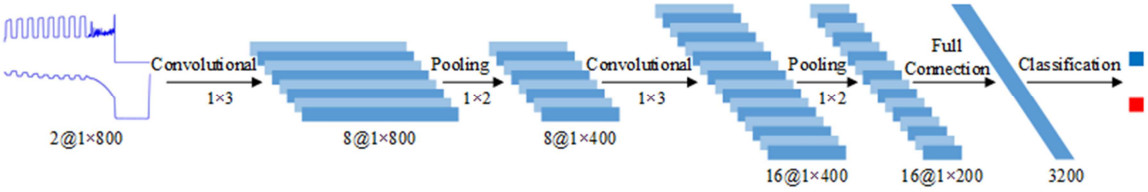

Figure 3. *CNN architecture.*

The CNN used in this paper comprises one input layer, two convolutional layers, two pooling layers, one full connection layer, and one output layer, as shown in Figure 3. The learning rate of the CNN is set to 0.001, and the number of iterations is set to 1200. After pre-processing the electrode position and current signals, an input layer of size 1 × 800 × 2 is used. The first convolutional layer comprises 8 convolutional cores with 1 × 3 size and 1 step size. The first pooling layer comprises 8 filters with 1 × 2 size and 1 step size. The second convolutional layer comprises 16 convolutional cores with 1 × 3 size and 1 step size. The second pooling layer comprises 16 filters with 1 × 2 size and 1 step size. The full connection layer comprises 3200 eigenvalues. Finally, the output layer divides the flash welding quality of the anchor chain into two categories: qualified and unqualified.

The convolutional kernel of the convolutional layer can be regarded as a sliding window in the time series, and the short-term features are extracted. The calculation formula for the convolutional layer is

$$x_j^l = f\left(\sum_{i \in M_j} x_i^{l-1} * k_{ij}^l + b_j^l\right) \tag{1}$$

where x_j^l is the jth eigenvector of the l layer, x_i^{l-1} is the ith eigenvector of the $l-1$ layer, M_j is the set of eigenvectors of the $l-1$ layer, $f(\square)$ is the activation function, "*" is the convolutional symbol, k_{ij}^l is the ith weighting coefficient of the layer l convolutional kernel j, and b_j^l is the offset coefficient corresponding to the jth convolution kernel of the l layer. k_{ij}^l and b_j^l are initialized to random values and adjusted to the best through network training.

The pooling layer performs the maximum pooling operation on the features acquired by the convolutional layer and retains useful information while reducing the amount of data. The calculation formula for the pooling layer is

$$y_j^l = f(\beta_j^l down(y_j^{l-1}) + c_j^l) \tag{2}$$

where y_j^l is the jth eigenvector of the l layer, y_i^{l-1} is the ith eigenvector of the $l-1$ layer, $down(\square)$ is a down-sampling function, β_j^l is the jth down-sampling coefficient of the l layer, and c_j^l is the jth bias coefficient of the l layer. β_j^l and c_j^l are initialized to random values and adjusted to the best through network training.

The calculation formula for the full connection layer is

$$z^l = f(W^l z^{l-1} + d^l) \tag{3}$$

where z^l is the eigenvector of the l layer, z^{l-1} is its eigenvector, W^l is its weight matrix, and d^l is its bias coefficient.

Dropout is used in the full connection layer to reduce the possibility of over-fitting. In the network training process, some nodes are randomly disabled, with their output values set to 0. The values of these nodes are recovered in the next network training process, and some nodes are randomly selected to repeat the process.

Dropout can avoid the over-fitting of some local features by the network and provide better generalization ability to CNN [16]. In the full connection layer, z^{l-1} is obtained by the following two formulas:

$$r^{l-1} \sim Bernoulli(p) \tag{4}$$

$$z^{l-1} = r^{l-1} \times z^{l-1} \tag{5}$$

Bernoulli randomly generates a vector r^{l-1} consisting of 0 and 1 with probability $P = 0.5$. The output value of 1 is reserved for the corresponding node, and that of the corresponding node of 0 is 0. Thus, a new z^{l-1} is obtained as the input of the full connection layer.

3. Data Pre-Processing and Experiments

3.1. Normalization

In deep learning, different evaluation indicators often have diverse dimensions and dimension units, affecting the results of data analysis. The data needs to be standardized to eliminate the dimensional influence on the indicators. This paper uses the min-max standardization method to normalize the electrode position and current signal. The formula is as follows:

$$x' = \frac{x - min}{max - min} \tag{6}$$

where *max* and *min* are the maximum and minimum values of the sample data. All data *x* are converted to x' between [0, 1]. The purpose is to eliminate the difference in the magnitude between the electrode position and the current signals, then avoid the error of network prediction caused by the large difference in the magnitude of input data.

3.2. Nearest-Neighbor Splicing Sampling

Because the number of qualified anchor chains is much larger than unqualified ones, the highly imbalanced data is a tricky issue in flash welding quality evaluation. Generally, there are three methods for addressing this issue: over-sampling for the minority class, under-sampling for the majority class, and synthesizing new data [17, 18].

The under-sampling method improves the classification accuracy of the minority class by reducing the number of majority samples. However, randomly discarded samples may abandon potentially useful information from the majority class, then reduce classification performance. The number of samples randomly increased by over-sampling the minority class. This method provides enough samples, but it

easily leads to over-fitting. This study analyzes the characteristics of anchor chain flash welding and proposes a new data synthesis method: the nearest-neighbor splicing sampling. The sampling flow is shown in Figure 4.

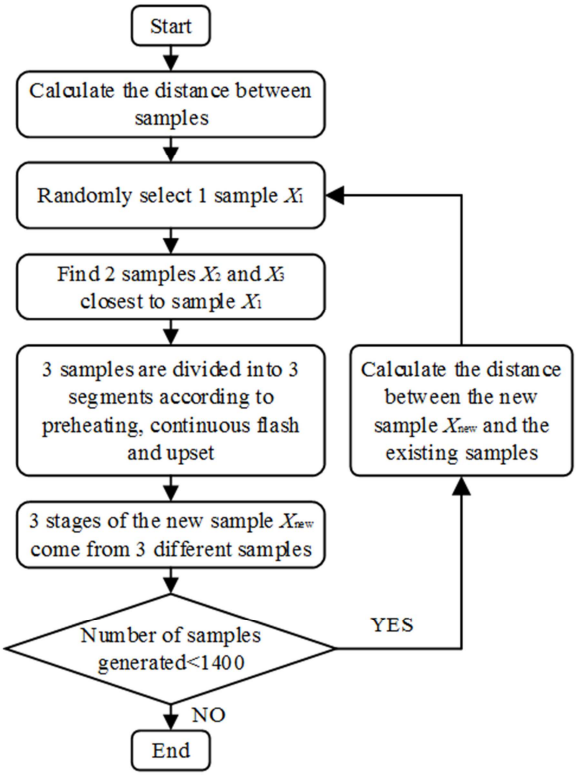

Figure 4. *Nearest-neighbour splicing sampling process.*

First, for each sample in the minority class, the dynamic time warping (DTW) distance is used to calculate its distance to other samples in the class [19, 20]. Assuming that A and B are two samples. Each sample contains electrode position and current signals, and the traditional DTW distance only applies to two one-dimensional time series. Thus, this paper makes some improvements to the multidimensional time series. The sample A can be expressed as $A_{electrode\ position} = \{a_1, a_2, \cdots, a_m\}$ and $A_{current} = \{a_1', a_2', \cdots, a_m'\}$, and those of the sample B can be expressed as $B_{electrode\ position} = \{b_1, b_2, \cdots, b_n\}$ and $B_{current} = \{b_1', b_2', \cdots, b_n'\}$. Construct the distance matrix D of m × n, and each element $d_{ij} = \|a_i - b_j\| + \|a_i' - b_j'\|$. A group of adjacent matrix elements is composed into a curved path, denoted as $W = \{w_1, w_2, \cdots, w_k\}$, whose kth element is $w_k = (d_{ij})_k$. This path satisfies the following conditions:

(1) $max\{m, n\} < k \le m + n - 1$;

(2) $w_1 = d_{11}$, $w_k = d_{mn}$;

(3) For $w_k = d_{ij}$ and $w_{k\text{-}1} = d_{i'j'}$, $0 \le i - i'$ and $0 \le j - j' \le 1$ must be satisfied.

The DTW distance can be summarised as using dynamic programming to find an optimal path with the minimum bending cost; that is,

$$\begin{cases} D(1,1) = d_{11} \\ D(i,j) = d_{ij} + min\{D(i,j-1), D(i-1,j), D(i-1,j-1)\} \end{cases} \tag{7}$$

where $i = 2, 3, \cdots, m$, $j = 2, 3, \cdots, n$, and the minimum cumulative value of the curved path in the matrix D is $D(m,n)$; then, the distance between sample A and sample B is

$$DTW(A,B) = D(m,n) \tag{8}$$

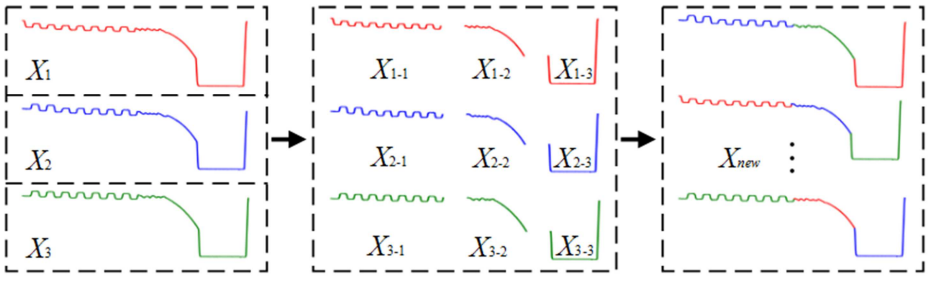

Figure 5. *Nearest-neighbor splicing sampling to generate new electrode location.*

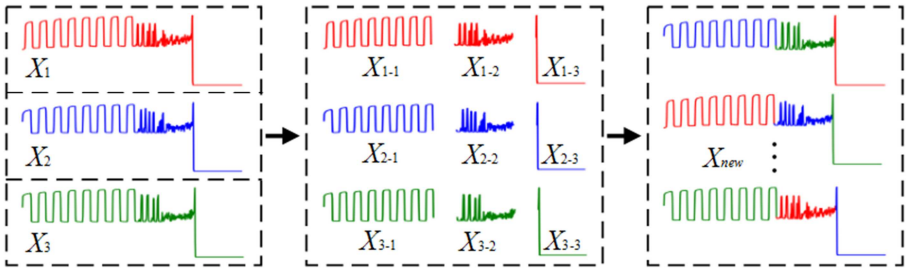

Figure 6. *Nearest-neighbor splicing sampling to generate new current.*

A sample X_1 is randomly selected from the minority class, and samples X_2 and X_3, which are closest to X_1, are also

selected. According to anchor chain flash welding characteristics, samples X_1, X_2, and X_3 are divided into three fragments: preheating, continuous flash, and upset. Three fragments, originating from different samples, are randomly selected and spliced into a new sample X_{new}. The splicing process is shown in Figures 5 and 6. The X_{new} is added to the unqualified sample set, and the distance between X_{new} and other samples is calculated. By continuously generating new samples from the unqualified sample set, the unqualified samples are expanded to 1500 groups.

The distance matrix is projected into the three-dimensional space to visualize the relationship between the samples, as shown in Figure 7. Figure 7 (a) shows the distance relationship between the original samples, and Figure 7 (b) shows the distance relationship after new samples are generated. The red circle indicates the unqualified anchor chain sample, the blue circle refers to the qualified anchor chain sample, and the green circle denotes the unqualified anchor chain sample generated using the nearest-neighbor splicing sample.

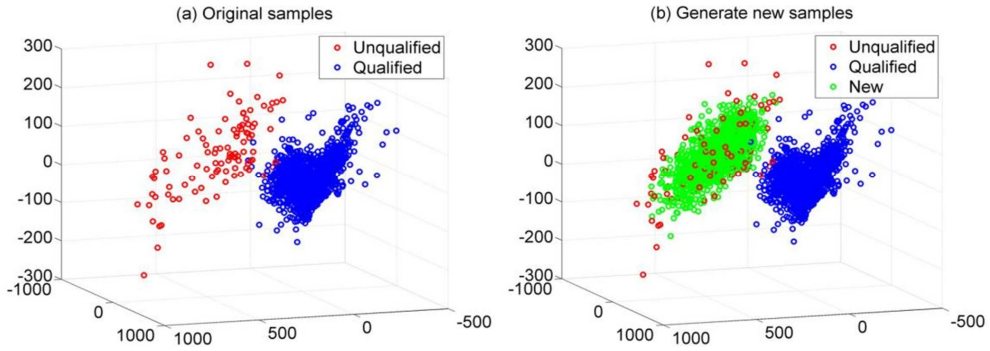

Figure 7. *Scatter plots before and after generating new samples.*

3.3. Piecewise Linear Interpolation

The input layer of the CNN requires the same data length. However, in real production, the time of anchor chain flash welding is affected by many factors. This paper adopts the piecewise linear interpolation method to interpolate the electrode position and current signals to handle this issue.

Piecewise linear interpolation is defined as follows: assuming that n + 1 interpolation nodes $a = x_0 < x_1 < \cdots < x_n = b$ and corresponding values $y_0, y_1, \cdots, y_n$ are given in the interval [a, b], n + 1 data points (x_i, y_i) on the plane can be obtained, and adjacent data points can be connected to form a line. The function $P(x)$, represented by n lines, is called the piecewise linear interpolation function of $x_0, x_1, \cdots, x_n$ with interval [a, b] [21]. The piecewise linear interpolation functions can be expressed as combinations of base functions:

$$P(x) = \sum_{i=0}^{n} l_i(x) y_i = l_0(x) y_0 + l_1(x) y_1 + \cdots + l_n(x) y_n \quad (9)$$

where $P(x)$ represents the interpolation function, $l_i(x)$ represents the interpolation base function, and y_i represents the value of the given function. The base functions are expressed as

$$l_0(x) = \begin{cases} \dfrac{x - x_1}{x_0 - x_1} & x \in [x_0, x_1] \\ 0 & x \in (x_1, x_n] \end{cases} \quad (10)$$

$$l_i(x) = \begin{cases} \dfrac{x - x_{i-1}}{x_i - x_{i-1}} & x \in [x_{i-1}, x_i] \\ \dfrac{x - x_{i+1}}{x_i - x_{i+1}} & x \in (x_i, x_{i+1}] \\ 0 & x \notin [x_{i-1}, x_{i+1}] \end{cases} \quad (11)$$

$$l_n(x) = \begin{cases} 0 & x \in [x_0, x_{n-1}) \\ \dfrac{x - x_{n-1}}{x_n - x_{n-1}} & x \in (x_{n-1}, x_n] \end{cases} \quad (12)$$

If $x \in [x_i, x_{i+1}]$, the piecewise linear interpolation function $P(x)$ can be expressed as

$$P(x) = \frac{x - x_{i+1}}{x_i - x_{i+1}} y_i + \frac{x - x_i}{x_{i+1} - x_i} y_{i+1} \quad (13)$$

Figures 8 and 9 show that the data lengths of red sample A and green sample B are different. Through piecewise linear interpolation of electrode position and current signals, not only the characteristics of the original signal are maintained but also the requirement of consistent input data length of the CNN is satisfied.

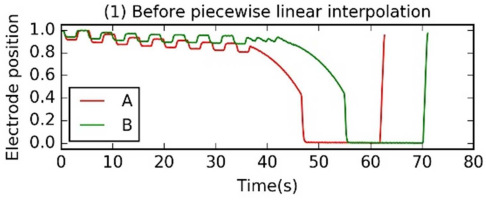

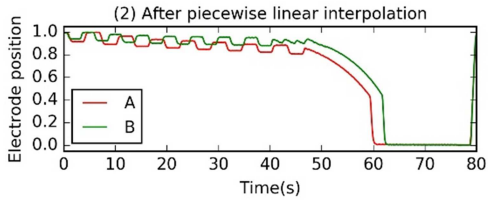

Figure 8. *Electrode position before and after piecewise linear interpolation.*

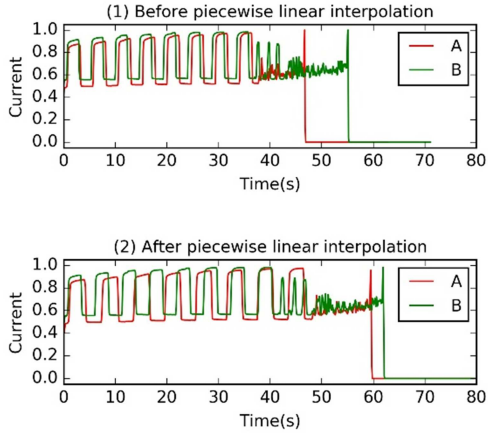

Figure 9. *Current before and after piecewise linear interpolation.*

3.4. Experimental Data

The experimental data used in this paper are the process signals collected from the flash welding process of the anchor chain. Sensors recorded the electrode position and current signals during welding, and a total of 1600 samples were collected, including 1500 qualified and 100 unqualified samples. To verify the superiority of the nearest-neighbor splicing sampling method proposed for solving the imbalanced dataset problem, the same CNN model is used to train and test the sample sets generated by under-sampling, over-sampling, and nearest-neighbor splicing sampling.

Under-sampling makes the number of samples equal to that of unqualified samples by extracting 100 samples from 1500 qualified samples. Over-sampling duplicates 100 unqualified samples to 1500, and nearest-neighbor splicing sampling balances the samples by generating 1400 new disqualified samples. Of the samples generated by the three methods, 80% were selected as the training set, and 20% were selected as the test set.

4. Results and Discussion

The CNN is used to train the three data processing methods for imbalanced dataset problems, and the loss value and accuracy of the training set are shown in Figures 10 and 11, respectively. As the number of iterations increases, the loss values of the three data processing methods tend to be stable and close to 0. The accuracy of the three methods is approximately 50% at the beginning. After continuous iterations, the accuracy finally reaches more than 90%. The accuracy of the under-sampling method, over-sampling method, and nearest-neighbor splicing sampling method are 93.8%, 95.9%, and 96.3%, respectively. In other words, the accuracy of our proposed method is the highest.

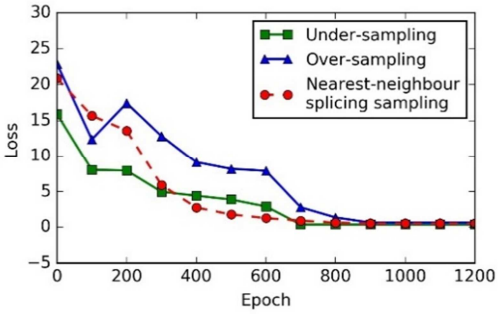

Figure 10. *Loss of the training set.*

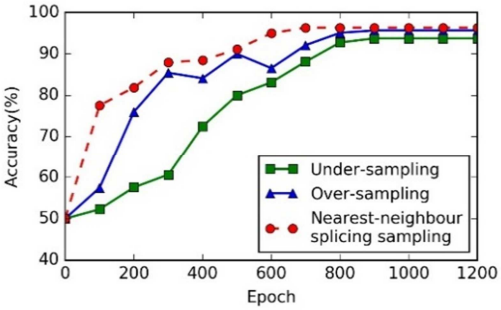

Figure 11. *Accuracy of the training set.*

This paper uses sensitivity, specificity, and accuracy as three indicators to evaluate the classification performance of CNN. Using the true positive (TP), true negative (TN), false positive (FP), and false negative (FN), these three indicators can be expressed as follows:

$$Sensitivity = \frac{TP}{TP + FN} \tag{14}$$

$$Specificity = \frac{TN}{TN + FP} \tag{15}$$

$$Accuracy = \frac{TP + TN}{TP + FN + TN + FP} \tag{16}$$

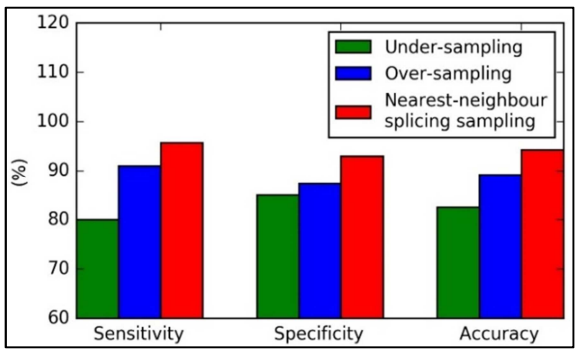

Figure 12. *Performance evaluation of the test set.*

Figure 12 shows the classification performance indicators of the test sets of the three data processing methods and the

relationship between the real and predicted labels, where the labels are divided into qualified and unqualified anchor chains. Sensitivity shows the percentage of qualified anchor chains correctly predicted, specificity displays the percentage of unqualified anchor chains correctly predicted, and accuracy shows the percentage of anchor chains correctly predicted.

The sensitivity, specificity, and accuracy of the under-sampling method in the test set are 80%, 85%, and 82.5%, respectively. The reduction of many qualified anchor chain samples took away useful information. The over-sampling method's sensitivity, specificity, and accuracy in the test set are 91%, 87.3%, and 89.2%, respectively. Simple replication of the unqualified anchor chain samples can easily lead to over-fitting, resulting in low test set accuracy.

The nearest-neighbor splicing sampling method proposed in this paper achieves the best prediction performance in the test set. The test set consists of 300 qualified and 300 unqualified anchor chains. The experimental results show that 287 anchor chains in the qualified anchor chain are predicted to be qualified, and 279 in the unqualified anchor chain are predicted to be unqualified. That is to say, the proposed method proposed in this paper effectively improves the accuracy of quality classification of anchor chain flash welding.

Table 1. *Performance comparison between CNN and SVM.*

Method	Sensitivity	Specificity	Accuracy
CNN	95.7%	93.0%	94.3%
SVM	93.3%	89.7%	91.5%

An SVM commonly used for time series classification is selected for comparison experiments to verify the accuracy of the CNN classification proposed in this paper. The experimental sample is the same as the CNN based on nearest-neighbor splicing sampling. The ratio of the training sample to the test sample is 4:1. Table 1 shows that the sensitivity, specificity, and accuracy of the SVM are 93.3%, 89.7%, and 91.5%, respectively, which are lower than those of the CNN. Compared with SVM, CNN is a deeper neural network that contains multiple convolutional and pooling layers. Thus, it is more conducive to the efficient classification of datasets.

5. Conclusions

This paper proposes a deep learning-based quality evaluation method for flash butt welding of anchor chains. A one-dimensional CNN model consisting of two convolutional layers, two pooling layers, and one full connection layer is employed to automatically learn the characteristics of electrode position and current signals during welding. The piecewise linear interpolation method is proposed to satisfy the requirement of consistent data length in the CNN's input layer. A novel method for solving the imbalanced dataset problem is presented: nearest-neighbor splicing sampling.

The experimental results show that the accuracy of nearest-neighbor splicing sampling on the test set is 94.3%, which is higher than that of under-sampling and over-sampling; the sensitivity, specificity, and accuracy of the 1D CNN model in the test set are 95.7%, 93%, and 94.3%, respectively, which are better than those of the SVM.

The proposed method can evaluate the quality of each anchor chain link, improving quality evaluation automation. The method has a good reference for similar practical problems, such as assessing the flash butt welding quality of automobile hubs and high-speed rail tracks.

Acknowledgements

This work is partly supported by the National Natural Science Foundation of China (Grant No. 51705214) and the National Quality Technology Infrastructure Construction Project of Zhejiang Quality Supervision System (Grant No. 20180129).

References

[1] D. Kim, W. So, and M. J. A. M. S. E. Kang, "Effect of flash butt welding parameters on weld quality of mooring chain," vol. 38, no. 2, pp. 112-117, 2009.

[2] S. Idapalapati, A. R. Akisanya, K. M. Loh, and S. J. E. F. A. Yeo, "Failure analysis of a failed anchor chain link," p. S1350630717310506, 2018.

[3] D. Li, D. Chen, J. Goh, and S. K. Ng, "Anomaly Detection with Generative Adversarial Networks for Multivariate Time Series," 2018.

[4] A. B. Nassif, I. Shahin, I. Attili, M. Azzeh, and K. Shaalan, "Speech Recognition Using Deep Neural Networks: A Systematic Review," IEEE Access, vol. 7, pp. 19143-19165, 2019.

[5] G. Pang, C. Shen, and A. Hengel, "Deep Anomaly Detection with Deviation Networks," in Knowledge Discovery and Data Mining, 2019.

[6] J. Zhang, Y. Xie, Q. Wu, and Y. Xia, "Medical image classification using synergic deep learning," Med Image Anal, vol. 54, pp. 10-19, May 2019.

[7] Y. Zhang, Y. Chen, J. Wang, and Z. Pan, "Unsupervised Deep Anomaly Detection for Multi-Sensor Time-Series Signals," 2021.

[8] J.-K. Park, W.-H. An, and D.-J. Kang, "Convolutional Neural Network Based Surface Inspection System for Non-patterned Welding Defects," International Journal of Precision Engineering and Manufacturing, vol. 20, no. 3, pp. 363-374, 2019.

[9] R. Du, Y. Xu, Z. Hou, J. Shu, and S. Chen, "Strong noise image processing for vision-based seam tracking in robotic gas metal arc welding," The International Journal of Advanced Manufacturing Technology, vol. 101, no. 5-8, pp. 2135-2149, 2018.

[10] M. Lngkvist, L. Karlsson, and A. J. P. R. L. Loutfi, "A review of unsupervised feature learning and deep learning for time-series modeling," vol. 42, pp. 11-24, 2014.

[11] C. A. Ronao and S. B. J. E. S. w. A. Cho, "Human activity recognition with smartphone sensors using deep learning neural networks," vol. 59, 2016.

[12] J. Zhao, X. Mao, and L. J. I. S. P. Chen, "Learning deep features to recognize speech emotion using merged deep CNN," vol. 12, no. 6, pp. 713-721, 2018.

[13] U. R. Acharya, H. Fujita, O. S. Lih, M. Adam, J. H. Tan, and C. K. J. K.-B. S. Chua, "Automated detection of coronary artery disease using different durations of ECG segments with convolutional neural network," Knowledge-Based Systems, vol. 132, no. sep. 15, pp. 62-71, 2017.

[14] X. Liu, Q. Zhou, J. Zhao, H. Shen, and X. Xiong, "Fault Diagnosis of Rotating Machinery under Noisy Environment Conditions Based on a 1-D Convolutional Autoencoder and 1-D Convolutional Neural Network," Sensors (Basel), vol. 19, no. 4, Feb 25 2019.

[15] H. Yang, C. Meng, and C. Wang, "Data-Driven Feature Extraction for Analog Circuit Fault Diagnosis Using 1-D Convolutional Neural Network," IEEE Access, vol. 8, pp. 18305-18315, 2020.

[16] S. Salman and X. Liu, "Overfitting Mechanism and Avoidance in Deep Neural Networks," ed, 2019.

[17] C.-F. Tsai, W.-C. Lin, Y.-H. Hu, and G.-T. Yao, "Under-sampling class imbalanced datasets by combining clustering analysis and instance selection," Information Sciences, vol. 477, pp. 47-54, 2019.

[18] X. Xu, W. Chen, and Y. Sun, "Over-sampling algorithm for imbalanced data classification," Jsee, vol. 30, no. 6, pp. 1182-1191, 2019.

[19] N. Dvornik, I. Hadji, K. G. Derpanis, A. Garg, and A. D. Jepson, "Drop-DTW: Aligning Common Signal Between Sequences While Dropping Outliers," in Neural Information Processing Systems, 2021.

[20] L. Wang and P. Koniusz, "Uncertainty-DTW for time series and sequences," in European Conference on Computer Vision, 2022, pp. 176-195: Springer.

[21] H. Wang, R. Pasupathy, B. W. J. A. T. o. M. Schmeiser, and C. Simulation, "Integer-ordered simulation optimization using RSPLINE: Retrospective search with piecewise-linear interpolation and neighborhood enumeration," Acm Transactions on Modeling and Computer Simulation, vol. 23, no. 3, pp. 1-24, 2013.